

**COUPLING FRESHLY ISOLATED CD44<sup>+</sup> INFRAPATELLAR FAT PAD DERIVED  
STROMAL CELLS WITH A TGF- $\beta$ 3 ELUTING CARTILAGE ECM-DERIVED  
SCAFFOLD AS A SINGLE STAGE **STRATEGY FOR PROMOTING  
CHONDROGENESIS****

*Henrique V. Almeida<sup>1,2</sup>, Gráinne M. Cunniffe<sup>1,2</sup>, Tatiana Vinardell<sup>3</sup>, Conor T. Buckley<sup>1,2</sup>, Fergal J. O'Brien<sup>1,4,5</sup>, Daniel J. Kelly<sup>1,2,5\*</sup>*

<sup>1</sup> Trinity Centre for Bioengineering, Trinity Biomedical Sciences Institute, Trinity College Dublin, Dublin 2, Ireland; <sup>2</sup> Department of Mechanical and Manufacturing Engineering, School of Engineering, Trinity College Dublin, Dublin 2, Ireland; <sup>3</sup> School of Agriculture and Food Science, University College Dublin, Belfield, Dublin 4, Ireland; <sup>4</sup> Department of Anatomy, Royal College of Surgeons in Ireland, Dublin 2, Ireland; <sup>5</sup> Advanced Materials and Bioengineering Research Centre (AMBER), Trinity College Dublin & RCSI, Dublin 2, Ireland

Corresponding author: Daniel J. Kelly, Ph.D.

Address: Department of Mechanical and Manufacturing Engineering, School of Engineering, Parson's Building Trinity College Dublin, Dublin 2, Ireland

Telephone: +353-1-896-3947, Fax: +353-1-679-5554

E-mail address: kellyd9@tcd.ie

**KEYWORDS:** articular cartilage, extracellular matrix, single-stage therapy, scaffold

## **ABSTRACT**

An alternative strategy to the use of *in vitro* expanded cells in regenerative medicine is the use of freshly isolated stromal cells, where a bioactive scaffold is used to provide an environment conducive to proliferation and tissue-specific differentiation *in vivo*.

The objective of this study was to develop a cartilage extracellular matrix (ECM) derived scaffold that could facilitate the rapid proliferation and chondrogenic differentiation of freshly isolated stromal cells. By freeze-drying cryomilled cartilage ECM of differing concentrations, it was possible to produce scaffolds with a range of pore sizes. The migration, proliferation and chondrogenic differentiation of infrapatellar fat pad derived stem cells (FPSCs) depended on the concentration/porosity of these scaffolds, with greater sGAG accumulation observed in scaffolds with larger sized pores. We then sought to determine if freshly isolated fat pad derived stromal cells, seeded onto a TGF- $\beta$ 3 eluting ECM-derived scaffold, could promote chondrogenesis *in vivo*. While a more cartilage-like tissue could be generated using culture expanded FPSCs compared to non-enriched freshly isolated cells, fresh CD44<sup>+</sup> stromal cells were capable of producing a tissue *in vivo* that stained strongly for sGAGs and type II collagen. These findings open up new possibilities for in-theatre cell based therapies for joint regeneration.

## 1. INTRODUCTION

Cartilage regeneration is still a major challenge in orthopaedic medicine. The outcomes of cartilage repair procedures are inconsistent and further joint degeneration commonly occurs.<sup>[1,2]</sup> Cell based therapies such as autologous chondrocyte implantation (ACI) may lead to improved clinical outcomes for patients, however the high cost and need for two hospital stays have limited the widespread adoption of this technique into the clinic.<sup>[3]</sup> This has motivated increased interest in single-stage or off-the-shelf therapies for cartilage regeneration, possibly involving the use of freshly isolated cells that can potentially be harvested in-theatre and delivered back into the patient during the same procedure.<sup>[4]</sup> Successful realization of such a concept therefore requires the identification of both a suitable cell source and the development of bioactive scaffolds capable of promoting the rapid proliferation and chondrogenic differentiation of the limited number of cells that can potentially be isolated from a patient in-theatre.

Extracellular matrix (ECM) derived from native tissue has been proposed as a promising biological scaffold material, providing cues that enhance cell proliferation, differentiation and matrix formation.<sup>[5,6]</sup> The ECM of articular cartilage is organized into a complex three-dimensional network, consisting primarily of type II collagen and proteoglycans in which growth factors and other cues are incorporated.<sup>[1,7]</sup> Devitalised and decellularized ECM-derived from articular cartilage has been used to produce bioactive scaffolds for cartilage tissue engineering applications.<sup>[5,7-10,11]</sup> These scaffolds have been shown to be chondro-inductive *in vitro*,<sup>[8]</sup> although their capacity to promote the development of functional hyaline cartilage is enhanced when additionally stimulated with exogenous growth factors such as transforming growth factor (TGF)- $\beta$ 3.<sup>[7,12]</sup> We have previously demonstrated that cartilage ECM-

derived scaffolds can also be used to control the delivery and release of TGF- $\beta$ 3 to stem cells,<sup>[7]</sup> opening up the potential of using such biomaterials as part of an off-the-shelf strategy for joint regeneration. While cartilage ECM is clearly a promising material for the development of scaffolds for cartilage tissue engineering applications, it is still unclear what the optimal composition and architecture (e.g. pore size) of such scaffolds should be to promote robust chondrogenesis. Given that such factors have been shown to play a key role in regulating cell fate in other scaffolding systems,<sup>[13,14]</sup> it would seem highly likely that scaffold composition and pore size would need to be tailored to promote the rapid proliferation and chondrogenic differentiation of any progenitor cell population intended to be used as part of a single-stage therapy for cartilage regeneration.

The overall goal of this study was to develop a single-stage **strategy** for **promoting chondrogenesis *in vivo* that combines** an optimised cartilage ECM-derived scaffold and freshly isolated infrapatellar fat pad derived stromal cells. The infrapatellar fat pad was chosen as a source of stromal cells as it is easily accessible to a clinician during joint repair procedures. Furthermore, infrapatellar fat pad derived stem cells (FPSCs) have been shown to have a strong chondrogenic potential and can be used to engineer functional cartilaginous grafts.<sup>[15,16]</sup> The objective of the first phase of the study was to develop cartilage ECM-derived scaffolds with controllable and consistent pore size and shape, and to then explore how altering their porosity influences the migration, proliferation and chondrogenic differentiation of human FPSCs that are seeded onto such constructs. We then explored the potential of such scaffolds to act as growth factor delivery systems to **facilitate** chondrogenesis of culture expanded FPSCs ***in vitro* and *in vivo***. Finally, we sought to determine if such

a scaffold could be coupled with enriched freshly isolated stromal cells as a one-step or single-stage **strategy** for **promoting chondrogenesis *in vivo***.

## **2. MATERIAL AND METHODS**

### **2.1. Scaffold preparation**

Cartilage used in the fabrication of ECM-derived scaffolds was harvested, under sterile conditions, from the femoral condyles and patella groove of three month old female pigs (n=3). The porcine breed from maternal side (50%) was: half Landrace, a quarter Duroc and a quarter Large White. The terminal side (50%) was: PIC Line 337. ECM was pooled before use. The cartilage was first sectioned into small pieces using a scalpel. These cartilage pieces were then fragmented using two different methods, to produce either “coarse” or “fine” scaffolds. Coarse scaffolds were produced using a previously described protocol,<sup>[7]</sup> where cartilage is blended in deionised water (dH<sub>2</sub>O) using an homogeniser (IKAT10, IKA Works Inc, NC, USA) to create a cartilage slurry. The homogenized tissue was centrifuged and the supernatant was removed. The remaining material was re-suspended in dH<sub>2</sub>O at a given concentration (500 mg ml<sup>-1</sup>).

Fine scaffolds were fabricated by first pulverising cartilage pieces within a cryogenic mill (6770 Freezer/Mill, SPEX, UK). These particles of cartilage were then blended in dH<sub>2</sub>O using a homogenizer (IKAT10, IKA Works Inc, NC, USA) to create a fine cartilage slurry. Three distinct scaffolds were fabricated using different slurry concentrations (250 mg ml<sup>-1</sup>; 500 mg ml<sup>-1</sup>; 1000 mg ml<sup>-1</sup>).

The slurry for both coarse and fine groups was transferred to custom made moulds (containing wells 5 mm in diameter and 3 mm in height) and freeze-dried (FreeZone Triad, Labconco, KC, USA) to produce porous scaffolds, as previously described.<sup>[7]</sup> Briefly, the slurry was frozen to -30°C (1°C min<sup>-1</sup>) and maintained at that

temperature for one hour. The temperature was then increased to  $-10^{\circ}\text{C}$  ( $1^{\circ}\text{C min}^{-1}$ ) and held for 24 hours before being increased to room temperature ( $0.5^{\circ}\text{C min}^{-1}$ ). Next, two different crosslinking techniques were applied to the scaffolds. The scaffolds underwent dehydrothermal (DHT) and 1-Ethyl-3-(3-dimethyl aminopropyl) carbodiimide (EDAC) crosslinking as previously described in literature.<sup>[7,17]</sup> The DHT process was performed in a vacuum oven (VD23, Binder, Germany), at  $115^{\circ}\text{C}$  and 2 mbar for 24 hours. The EDAC (Sigma-Aldrich, Germany) crosslinking consisted of chemical exposure (2 hours; 6 mM) in the presence of N-Hydroxysuccinimide (NHS) (Sigma-Aldrich, Germany), a catalyst that is commonly used with EDAC. A molar ratio of 2.5 M EDAC/M N-Hydroxysuccinimide was used.<sup>[17,18]</sup>

## **2.2. Helium ion microscopy (HIM) and Light Microscopy**

Devitalized ECM-derived scaffolds were imaged using Helium ion microscopy (HIM) (Zeiss Orion Plus, Germany) as previously described.<sup>[7]</sup> Image resolution of the microscope was 0.35 nm, with a working distance of 10 mm and a 10  $\mu\text{m}$  aperture. Beam current was 0.8 pA with a tilt angle of  $15^{\circ}$ . Charge compensation was enabled using an electron beam flood gun. No conductive coating of the specimens was employed. The main goal of this step was to confirm and compare scaffold porosity between the different groups. Routine light microscopy was also used for morphometrical and histological analysis.

## **2.3. Diameter, particle size, pore size determination and mechanical testing**

After the 4 weeks culture period, constructs were removed from culture wells and imaged. Macroscopic images were analyzed with Image J to quantify changes in construct diameter ( $n=4$ ) and particle size. As previously described, pore size

determination for the scaffolds was obtained by measuring the diameter of 40 pores (with Image J) in HIM micrographs of dry scaffolds (n=3) before cell seeding.<sup>[19]</sup>

Scaffolds were mechanically tested dry using a standard materials testing machine with a 5 N load cell (Zwick Z005, Roell, Germany).<sup>[16]</sup> A preload of 0.03N was applied to ensure direct contact between the scaffold and the loading platens. A ramp compressive strain of 10% was applied to samples, from which the Young's modulus was determined from the slope of the stress-strain curve. Engineered tissues at day 28 were tested using a similar protocol, except constructs were hydrated and maintained in a bath of phosphate buffered saline (PBS) (Sigma-Aldrich, Germany).

#### **2.4. Cell culture**

Ethical approval for the isolation of human FPSCs was obtained from the institutional review board of the Mater Misericordiae University Hospital, Dublin, Ireland. Cells were isolated from the infrapatellar fat pad of patient (Female, diseased donor, age 52) undergoing total joint arthroplasty. The fat pad was harvested, weighed and washed thoroughly in PBS (Sigma-Aldrich, Germany). Next, the tissue was diced in sterile conditions followed by rotation at 37°C in high-glucose Dulbecco's Modified Eagle Medium (hgDMEM, GlutaMAX™)(GIBCO, Biosciences, Ireland) containing collagenase type II (750 U ml<sup>-1</sup>, Worthington Biochemical, LaganBach Services, Ireland) and 1% penicillin (100 U ml<sup>-1</sup>)-streptomycin (100 µg ml<sup>-1</sup>) for approximately 4 hours. A ratio of 4 ml of collagenase (750 U ml<sup>-1</sup>) per gram of tissue was found to be optimal based on previous work.<sup>[20, 21]</sup> After digestion, cells were washed, filtered (40 µm nylon cell strainer) and centrifuged (650 g; 5 minutes). The supernatant was removed. The remaining cells were re-suspended, counted and finally plated (5000 cells cm<sup>-2</sup>) in T-175 flasks (Sarsted, Wexford, Ireland). Cells

were cultured in a standard media formulation, which consisted of hgDMEM containing 10% foetal bovine serum and 1% penicillin (100 U ml<sup>-1</sup>)-streptomycin (100 mg ml<sup>-1</sup>) (GIBCO, Biosciences, Ireland) with the addition of fibroblast-growth factor-2 (FGF-2, 5 ng ml<sup>-1</sup>; ProSpec-Tany TechnoGene Ltd, Israel). Cells were expanded to passage 2 (P2), with an initial seeding density of 5000 cells cm<sup>-2</sup> at each passage. Media changes were performed twice weekly.

For *in vitro* studies, each scaffold was seeded with 0.5x10<sup>6</sup> human FPSCs. Constructs were maintained in chemically defined chondrogenic medium (CDM), as previously described, for 28 days (5% O<sub>2</sub>; 37°C).<sup>[21]</sup> CDM consisted of DMEM GlutaMAX<sup>TM</sup> supplemented with penicillin (100 U ml<sup>-1</sup>)-streptomycin (100 µg ml<sup>-1</sup>) (both GIBCO, Biosciences, Ireland), sodium pyruvate (100 µg ml<sup>-1</sup>), L-proline (40 µg ml<sup>-1</sup>), L-ascorbic acid-2-phosphate (50 µg ml<sup>-1</sup>), bovine serum albumin (BSA) (1.5 mg ml<sup>-1</sup>), insulin-transferrin-selenium (1x), dexamethasone (100 nM) (all from Sigma-Aldrich, Ireland) and recombinant human transforming growth factor-β3 (TGF-β3; ProSpec-Tany TechnoGene Ltd, Israel) (10 ng ml<sup>-1</sup>). Groups termed “loaded with TGF-β3” were not supplemented with TGF-β3 in chondrogenic media during the culture period. Instead, TGF-β3 (approximately 5 ng in 40 µl of media) was soak-loaded into the scaffold and was not directly added to the culture media. The scaffolds were maintained in 12 well plates and each scaffold was placed within cylindrical agarose moulds. After seeding, the scaffolds with the cells plus CDM (40 µl) were left in the incubator for two hours. After two hours, supplemented CDM (2.5 ml) was added to each well. Media changes were performed twice weekly. The media was stored (-85°C) for further analysis.



## 2.5. Biochemical analysis

Constructs were biochemically analyzed at day 0 and 28, for DNA content, sulphated glycosaminoglycan (sGAG) and collagen content, as previously described.<sup>[16]</sup> Briefly, constructs were enzymatically digested by incubation in papain (125  $\mu\text{g ml}^{-1}$ ) in sodium acetate (0.1 M), cysteine HCl (5 mM), Ethylenediaminetetraacetic acid (EDTA) (0.05 M), pH 6.0 (all from Sigma-Aldrich, Ireland) at 60°C under rotation (10 rpm; 18 hours). As previously described, DNA content of each sample was quantified using the Hoechst Bisbenzimidazole 33258 dye assay, with a calf thymus DNA standard.<sup>[19]</sup> The proteoglycan content was estimated by quantifying the sGAG in constructs using the dimethylmethylene blue dye-binding assay (Blyscan, Biocolor Ltd., Northern Ireland), using bovine chondroitin sulphate as a standard. Collagen content in the constructs was quantified by measuring hydroxyproline content, after acidic hydrolysis of the samples (110°C; 18 hours) in concentrated HCl (38%). Samples were assayed using a chloramine-T assay assuming a hydroxyproline/collagen ratio of 1:7.69.<sup>[20]</sup>

## 2.6. Cell viability and distribution

Cell survival and distribution were assessed using live/dead staining for all slurry concentrations. Calcein was used to stain live cells and images were taken using confocal microscopy after 2 hours of culture, as previously described.<sup>[19]</sup> Briefly, at day 1 and 28, cell viability was assessed by LIVE/DEAD<sup>®</sup> kit (Invitrogen, Bio-science, Ireland). Constructs were washed in PBS, sectioned in half, incubated in calcein (2  $\mu\text{M}$ ) (live/green) and ethidium homodimer-1 (4  $\mu\text{M}$ ) (dead/red) (Cambridge Biosciences, UK). Constructs were washed again and imaged in confocal microscope 10x Olympus FV-1000 Point-Scanning Microscope (Southend-

on-Sea, UK) at 515 and 615 nm channels and analysed using FV10-ASW 2.0 Viewer.

## 2.7. Histology and immunohistochemistry

Constructs were fixed overnight (4°C) in a solution of paraformaldehyde (4%) (Sigma-Aldrich, Ireland), followed by washing in PBS (Sigma-Aldrich, Ireland), dehydrated and wax embedded. Wax embedded constructs were sectioned to produce 6 µm thick slices and mounted on microscope slides. Sections were stained with 1% alcian blue 8GX (Sigma-Aldrich) in HCl (0.1 M) for sGAG and with picrosirius red for collagen. Cell *nuclei* were also stained with 0.1% nuclear fast red solution (Sigma-Aldrich). With the aim of monitoring the newly formed sGAG, constructs were histologically analysed (alcian blue) at day 0, 7, 14 and 28. As previously described,<sup>[21]</sup> immunohistochemical analysis was performed on 6 µm sections using monoclonal antibody to type II collagen (Abcam, UK). Samples were washed in PBS and subjected to peroxidase activity (20 minutes), incubated (1 hour, 37°C in a moist environment) with chondroitinase ABC (Sigma, 0.25 U ml<sup>-1</sup>) with the aim of enhancing the permeability of the ECM by removing the chondroitin sulphate. Slides were rinsed with PBS and blocked with 10% goat serum (30 minutes) and incubated with mouse monoclonal anti-collagen type II diluted 1:100 (1 mg ml<sup>-1</sup>; 1 hour at RT) (Abcam, UK). A secondary antibody for type II collagen (1 mg ml<sup>-1</sup>; 1 hour) (Anti-Mouse IgG Biotin antibody produced in goat) binding was then applied. By using Vectastain ABC reagent (Vectastain ABC kit, Vector Laboratories, UK) for 5 minutes in peroxidase DAB substrate kit (Vector laboratories, UK), it was possible to observe a colour alteration. Samples were dehydrated with graded ethanol and xylene and mounted with Vectamount medium (Vector Laboratories, UK). Positive

and negative controls (porcine cartilage and ligament) were included in the immunohistochemistry staining protocol for each batch.<sup>[16]</sup>

## **2.8. ELISA - TGF- $\beta$ 3 release to the media**

The amount of TGF- $\beta$ 3 release from the growth factor loaded cartilage ECM-derived scaffold was determined via ELISA, as previously described<sup>[7,22]</sup>. 96 well plates were coated with capture antibody ( $360 \mu\text{g ml}^{-1}$ ) with mouse anti-human TGF- $\beta$ 3 (R&D Systems, UK). The samples (8 time points) and TGF- $\beta$ 3 standards (ProSpec-Tany TechnoGene Ltd, Israel) were incubated for 2 hours. After washing and drying, detection antibody ( $18 \mu\text{g ml}^{-1}$  of biotinylated goat anti-human TGF- $\beta$ 3) was added to the plate and incubated (2 hours). The next step was to wash, dry and incubate the plate in streptavidin-HRP (horseradish-peroxidase) (R&D Systems, UK) for 20 minutes in the dark. Substrate solution (1:1 mixture of  $\text{H}_2\text{O}_2$  and tetramethylbenzidine; R&D Systems, UK) was added to each well, followed by incubation (20 minutes) avoiding direct light. Stop solution (2 N  $\text{H}_2\text{SO}_4$ ; Sigma-Aldrich, Germany) was added and the optical density was determined immediately with a plate reader set to 450 nm.

## **2.9. *In vivo* and cell population enrichment**

ECM-derived (DHT+EDAC crosslinked) scaffolds loaded with 5 ng of TGF- $\beta$ 3 were seeded as follow: 1. No cells; 2. monolayer expanded (Passage 2) FPSCs; 3. FPSCs; 4. CD44<sup>+</sup> FPSCs. All cells were isolated from porcine (female, 3 month old) infrapatellar fat pad and each scaffold was seeded with  $0.5 \times 10^6$  cells, with the exception of CD44<sup>+</sup> where the number was  $0.1 \times 10^6$  (approximately 10% of the freshly isolated fraction). CD44<sup>+</sup> cells were isolated using magnetic-activated cell sorting (MACS<sup>®</sup>, Miltenyi Biotec, Germany). Briefly, CD44<sup>+</sup> cells were labelled with

micro-beads specific to CD44 according to the manufacturer's instructions. This cell suspension was then passed through a MACS column in a magnetic field. Magnetically labelled cells CD44<sup>+</sup> cells can be separated after removing the magnet. Within 24 hours of cell isolation, seeded constructs were subcutaneously implanted into nude mice.

Constructs (n=6) were implanted into the back of nude mice (Female, 6 weeks old, Balb/c; Harlan), with an n=9 per group. Mice were weighed and anesthetized with an intraperitoneal injection of xylazine (10 mg kg<sup>-1</sup>) (Chanazine 2%; Chanelle) and ketamine (100 mg kg<sup>-1</sup>) (Narketan; Vetoquinol). Skin incisions were made along the central line of the spine. Three constructs were inserted in each subcutaneous pocket, and sutured using 4-0 Vicryl plus (Ethicon, Johnson & Johnson) and tissue glue (Vetloc xcel). Euthanasia was performed 4 weeks after the surgery by CO<sub>2</sub> inhalation (confirmed by cervical dislocation), and the constructs were analyzed histologically, immunohistochemically, and biochemically. The protocol was reviewed and approved by Trinity College Dublin ethics committee.

## **2.10. Statistical analysis**

Results are presented as mean ± standard deviation. Statistical analysis was performed with MINITAB 15.1 software package (Minitab Ltd., Coventry, UK). Experimental groups were analyzed for significant differences using a general linear model for analysis of variance (ANOVA) with factors including concentration, crosslinking technique and growth factor supplementation. Tukey's test for multiple comparisons was used to compare conditions. Significance was accepted at a level of  $p < 0.05$ .

### 3. RESULTS

#### 3.1. Chondro-permissive scaffolds with a consistent structure and pore size can be produced using cryomilled cartilage extracellular matrix (ECM)

Scaffold pore size has been shown to regulate stem cell proliferation and differentiation.<sup>[13,23]</sup> Hence, we first sought to develop a method to produce scaffolds from cartilaginous ECM with controllable and consistent pore size and shape. Porous scaffolds were produced using slurries of either coarse (ECM blended using a homogeniser) (**Figure 1A**) or fine (cryomilled ECM) porcine cartilage ECM (**Figure 1B**). The coarse ECM slurry contained particles with a mean size of  $322\pm 195\ \mu\text{m}$ , while the fine slurry contained particles with a mean pore size of  $97\pm 26\ \mu\text{m}$ . Large cartilage particles were still present in the freeze-dried scaffold fabricated using the coarse slurry (**Figure 1C**), while a scaffold with a more homogenous pore size and morphology was produced using the fine particulated cartilage ECM slurry (**Figure 1D**). This was confirmed using helium ion microscopy, where more homogenous and spherical pores (mean diameter -  $65\pm 20\ \mu\text{m}$ ) were observed in the fine ECM scaffolds (**Figure 1F**), whilst less spherical pores and a wider distribution of pore sizes (mean diameter -  $104\pm 49\ \mu\text{m}$ ) was observed in the coarse ECM scaffolds (**Figure 1E**).

We next sought to compare the capacity of both coarse and fine cartilage ECM-derived scaffolds to promote chondrogenesis of human FPSCs. Tissues engineered using both coarse and fine ECM-derived scaffolds stained similarly for sGAG and collagen deposition after 28 days in culture (**Figure 2A, B**). There was no significant difference in the sGAG and collagen content of tissues engineered using the two different scaffold types (data not shown).

### **3.2. The porosity of cartilage ECM-derived scaffolds can be tailored by varying the concentration of the slurry**

As the fine (or cryomilled) cartilage ECM particles could be used to produce scaffolds with a consistent pore size and shape, we next sought to determine how the concentration of such slurries would influence the pore size of the resulting scaffolds. HIM demonstrated that varying the ECM slurry concentration (250, 500 and 1000 mg ml<sup>-1</sup>) led to the development of scaffolds with different pore sizes (**Figure 3**). Specifically, lowering the concentration of ECM led to the development of scaffolds with a higher mean pore size (from 32±12 µm to 65±20 µm; **Figure 3D**). The bulk compressive modulus of the dry scaffolds increased with ECM concentration (**Figure 3E**); although they become noticeably softer when hydrated. The sGAG content of the 250, 500 and 1000 mg ml<sup>-1</sup> scaffold was 58.5±6.5 µg, 191.0±8.0 µg, and 230.0±11.0 µg respectively; while the residual DNA content of the 250, 500 and 1000 mg ml<sup>-1</sup> scaffold was 11.0±1.0 µg, 25.0±1.0 µg and 38.0±7.0 µg respectively.

### **3.3. Stem cell migration, proliferation and chondrogenic differentiation depends on the porosity of ECM-derived scaffolds**

FPSCs were then seeded onto scaffolds fabricated using a range of slurry concentrations/pore sizes to determine their capacity to facilitate FPSC migration, proliferation and subsequent chondrogenesis. Confocal microscopy revealed that FPSCs were evenly distributed throughout the 250 mg ml<sup>-1</sup> scaffolds after 1 day of culture (**Figure 4A**), while cells were only observed around the periphery of the lower pore size 500 and 1000 mg ml<sup>-1</sup> scaffolds (**Figure 4B, C**). After 28 days of culture, FPSCs were observed throughout the majority of the 250 and 500 mg ml<sup>-1</sup> scaffolds, except for a region in the very centre of the 500 mg ml<sup>-1</sup> scaffold, while viable cells

were only observed around the periphery of the 1000 mg ml<sup>-1</sup> scaffolds. Greater FPSC proliferation was also observed within the 250 mg ml<sup>-1</sup> scaffolds, as evidenced by a significant increase in DNA content (164%,  $p < 0.05$ ) within this scaffold over 28 days in culture, whilst no significant change in DNA content was observed in the 500 and 1000 mg ml<sup>-1</sup> scaffolds.

Histological analysis (nuclear fast red *nuclei* staining) on day 0, 7, 14 and 28 of culture confirmed that FPSCs were homogeneously distributed throughout the 250 mg ml<sup>-1</sup> scaffold (**Figure 5A**). Furthermore, robust proteoglycan deposition was observed throughout this construct by day 28 (**Figure 5A, D**). In contrast, the lower pore sized 1000 mg ml<sup>-1</sup> scaffolds stained less intensely and more inhomogeneously for Alcian Blue compared to other constructs. This was confirmed by biochemical analysis of the sGAG content of the engineered tissues, which demonstrated greater levels of ECM accumulation within the 250 mg ml<sup>-1</sup> scaffolds (**Figure 5**). The greater levels of cellular infiltration and proliferation within the lower concentration scaffolds (Figure 4, 5) likely contribute to these higher levels of sGAG accumulation. In addition, the 250 mg ml<sup>-1</sup> constructs were stiffest after 28 days in culture (**Figure 5F**). Based on these results, the 250 mg ml<sup>-1</sup> fine scaffold was selected for further development in the remainder of the study.

### **3.4. EDAC crosslinking of ECM-derived scaffolds prevented cell mediated contraction with no loss in chondro-inductive capacity**

A potential limitation of the lower concentration cartilage ECM-derived scaffolds was that they underwent greater levels of contraction during culture compared to higher concentration scaffolds (data not shown). Previous studies have demonstrated that EDAC crosslinking is an efficient way to minimize cell mediated contraction in scaffolds for cartilage tissue engineering applications.<sup>[5,7]</sup> Therefore,

250 mg ml<sup>-1</sup> scaffolds were physically crosslinked using DHT and chemically with EDAC. Significantly less contraction was observed in scaffolds that underwent both EDAC and DHT crosslinking (**Figure 7A, B**). The diameter of the EDAC crosslinked scaffolds did not change over 28 days in culture, and was significantly higher than the DHT only crosslinked scaffolds.

The next step was to assess and confirm that the chondro-inductivity of the scaffolds was not affected by the use of EDAC crosslinking. Histological analysis revealed that robust levels of cartilage ECM deposition occurred within both EDAC plus DHT (**Figure 7B**) and DHT only (**Figure 7A**) crosslinked scaffolds. Furthermore, the sGAG content of DHT plus EDAC scaffolds was significantly higher than that of DHT only constructs (**Figure 7C**), confirming that EDAC crosslinking does not suppress chondrogenesis within cartilage ECM-derived scaffolds.

### **3.5. EDAC crosslinking delays the burst release of TGF- $\beta$ 3 from cartilage ECM-derived scaffolds**

We have previously demonstrated that cartilage ECM-derived scaffolds (derived from coarse ECM particles) can be used as platforms to control the release of soak loaded growth factor and consequently induce robust chondrogenesis of FPSCs.<sup>[7]</sup> To confirm that cartilage ECM-derived scaffolds derived from a slurry of fine particles can also be used to control the release of exogenously supplied TGF- $\beta$ 3, and to evaluate the impact of EDAC crosslinking on growth factor release, an ELISA was performed to determine the release of TGF- $\beta$ 3 into the media (**Figure 8B**). After 4 days of culture, the media of the EDAC plus DHT crosslinked scaffolds contained significantly lower levels TGF- $\beta$ 3 compared to the DHT-only crosslinked scaffold. Both scaffolds released almost all of the TGF- $\beta$ 3 loaded onto the scaffold within the first 10 days of the culture period.



The next goal was to confirm that loading of TGF- $\beta$ 3 onto the scaffold could induce at least comparable chondrogenesis to directly supplementing the culture media with this growth factor. Both the DHT and DHT plus EDAC crosslinked scaffolds that were soak loaded with TGF- $\beta$ 3 were capable of inducing robust chondrogenesis of FPSCs, as evidenced by alcian blue, picro-sirius red and type II collagen immunohistochemical staining (**Figure 8A, B**). The sGAG content of constructs after 28 days of culture was higher for DHT crosslinked scaffolds when soak loaded with TGF- $\beta$ 3 (**Figure 8A**) compared to scaffolds where the media was directly supplemented with TGF- $\beta$ 3. A similar trend was observed for DHT plus EDAC crosslinked scaffolds (**Figure 8A**).

### **3.6. Coupling freshly isolated CD44<sup>+</sup> infrapatellar fat pad derived stromal cells with a TGF- $\beta$ 3 eluting cartilage ECM-derived scaffold promotes chondrogenesis *in vivo***

We next sought to evaluate whether a TGF- $\beta$ 3 eluting cartilage ECM-derived scaffold, optimized *in vitro* to promote stem cell proliferation and chondrogenic differentiation, could be used to promote chondrogenesis of culture expanded FPSCs *in vivo*. To this end, cell-free and FPSC-loaded constructs were implanted subcutaneously into nude mice. After 28 days *in vivo*, cell free scaffolds had been infiltrated with host cells that synthesised a fibrous or fibrocartilaginous tissue. The pores of ECM-derived scaffolds seeded with culture expanded FPSCs stained more intensely for glycosaminoglycan (Alcian Blue) and type II collagen deposition compared to cell-free constructs (**Figure 9C, D**). With the ultimate objective of developing a single-stage therapy for articular cartilage regeneration, we next sought to determine if freshly isolated (i.e. not culture expanded) infrapatellar fat pad derived stromal cells, seeded into the same TGF- $\beta$ 3 eluting cartilage ECM-derived scaffold,

could be used as an alternative to culture expanded FPSCs to promote chondrogenesis *in vivo*. The tissue formed in constructs seeded with freshly isolated FPSCs was comparable to that within cell-free constructs, suggesting that this cell population was not capable of undergoing robust chondrogenesis within the scaffolds *in vivo*. Given that the infrapatellar fat pad contains a heterogeneous cell population, we finally sought to determine if freshly isolated CD44<sup>+</sup> (a putative marker of chondro-progenitors) fat pad derived stromal cells would promote more robust chondrogenesis *in vivo*. Cartilage-like matrix deposition was observed throughout CD44<sup>+</sup> cell seeded constructs, with localized regions staining intensely for sGAG and type II collagen deposition (**Figure 9I, J**).

#### **4. DISCUSSION**

The overall goal of this study was to develop a single-stage **strategy for promoting chondrogenesis *in vivo* consisting of** an optimised cartilage ECM-derived scaffold and freshly isolated infrapatellar fat pad derived stromal cells. By freeze-drying slurries of cryomilled cartilage ECM of differing concentrations, it was possible to produce scaffolds with a range of pore sizes. The migration, proliferation and chondrogenic differentiation of FPSCs depended on the concentration/porosity of the ECM-derived scaffolds, with greater sGAG accumulation observed within the scaffolds with a larger pore size. A limitation of these more porous scaffolds was that they underwent greater cell-mediated contraction. However this could be prevented with the use of combined dehydrothermal (DHT) and 1-Ethyl-3-(3-dimethylaminopropyl) carbodiimide (EDAC) crosslinking, with no loss in scaffold chondro-inductive capacity. Such crosslinking also functioned to retard the initial release of exogenously loaded TGF- $\beta$ 3 from stem cell seeded scaffolds. Finally, the optimized scaffold was seeded either with culture expanded FPSCs or freshly isolated

infrapatellar fat pad derived stromal cells and implanted subcutaneously into nude mice. The results of this study demonstrate that a cartilage ECM-derived scaffold loaded with TGF- $\beta$ 3 supports cartilage-like tissue formation *in vivo*, specifically when seeded with culture expanded FPSCs or freshly isolated CD44<sup>+</sup> stromal cells. These findings open up the possibility of using freshly isolated CD44<sup>+</sup> stromal cells from the infrapatellar fat pad of the knee as part of a single-stage therapy for joint regeneration.

Freeze-drying slurries of fine (cryomilled) cartilage ECM particles was found to result in the development of scaffolds with a consistent pore size and morphology. Similar strategies have been employed in the literature to particulate ECM.<sup>[24]</sup> From a translational perspective, the identification of robust and consistent strategies for scaffold fabrication will be important, for example, by leading to the development of production methods that minimise batch-to-batch variability. In addition, modifying ECM particles size may also influence the efficacy of the resulting scaffold to facilitate tissue regeneration. For example, previous studies have demonstrated that the particle size of powdered ECM material can influence new tissue forming fate, despite the fact that similar proteins were found in both biomaterials.<sup>[25]</sup> In the current study, the chondro-inductive properties of cartilage ECM-derived scaffold were found to be independent of particle size, i.e. it was similar for both coarse and fine cartilage ECM-derived scaffolds. What remains unclear at this stage is how the devitalization and scaffold fabrication process affects the composition of the ECM (e.g. sGAG and collagen content relative to native tissue). In addition, while the devitalization process used in this study will disrupt cellular structures, DNA and other cellular components that remain within the ECM that may elicit an immune response *in vivo*. Further work needs to be done to determine immunogenicity of chondral ECM-derived

materials,<sup>[11]</sup> and to optimise the decellularization of such matrices to facilitate their clinical translation.

Reducing the ECM concentration led to the development of scaffolds with a larger pore size, which in turn enhanced cellular infiltration, proliferation and chondrogenic differentiation. Previous studies have also reported that the porosity of ECM-derived scaffolds depend on slurry ECM concentration.<sup>[9]</sup> It is still unclear as to what the ideal scaffold pore size is for facilitating cell attachment, proliferation and migration in tissue engineering, with a wide range (5 to 500  $\mu\text{m}$ ) utilized in the literature depending on the cell type.<sup>[26]</sup> In the context of stem cell differentiation, it has been demonstrated that chondrogenesis is enhanced in poly ( $\epsilon$ -caprolactone) (PCL) scaffolds with a larger pore size.<sup>[27]</sup> Within osteochondral defects, it has been demonstrated that cell-seeded poly(lactide-co-glycolide) (PLGA) scaffolds with 100-200  $\mu\text{m}$  pores in the chondral layer and 300-450  $\mu\text{m}$  pores in the osseous layer best supported joint regeneration.<sup>[28]</sup> In addition to pore size, scaffold stiffness has also been shown to regulate stem cell differentiation, with softer scaffolds shown to support chondrogenesis, and stiffer scaffolds shown to support osteogenesis.<sup>[17]</sup> Therefore the enhanced chondrogenesis observed in the higher porosity/lower concentration ECM-derived scaffolds observed in this study may be due, at least in part, to alterations in scaffold stiffness as the concentration of the scaffold is reduced. Additional mechanical testing on individual scaffold struts is required to further test this hypothesis. Scaffold composition can also influence its degradation kinetics and hence the release rates of biochemical cues,<sup>[29]</sup> which could also contribute to the altered levels of chondrogenesis observed in different concentration/porosity ECM-derived scaffolds.

In agreement with previous studies, we found that EDAC crosslinking prevented contraction of cartilage ECM-derived scaffolds.<sup>[7]</sup> It was also found that sGAG accumulation was greater within EDAC plus DHT crosslinked scaffolds compared with the DHT only scaffolds, likely due to superior sGAG retention within this construct. Further *in vivo* studies are also necessary to examine other impacts of EDAC, including the immunological response.<sup>[24]</sup>

A further impact of EDAC crosslinking was the delay in the initial release of TGF- $\beta$ 3 from the scaffold. Previous studies have demonstrated that altering the degree of crosslinking of collagen-like micro-spheres affects the release profile of growth factors such as TGF- $\beta$ .<sup>[30]</sup> Irrespective of the degree of scaffold crosslinking, the majority of the growth factor was released from the ECM-derived scaffolds within the first 10 days of culture. Superior chondrogenesis was also observed in scaffolds loaded with TGF- $\beta$ 3 compared to constructs where the growth factor was directly added to the media, despite the fact that a much lower amount of TGF- $\beta$ 3 was soaked onto these scaffolds (5ng) compared to what was added to the media over the 4 week culture period (~200ng). This may be explained by the temporal release of TGF- $\beta$ 3 from the scaffold, as a number of studies have demonstrated that short-term exposure to growth factors enhances chondrogenesis.<sup>[31]</sup> These results provide further support for the concept that ECM-derived scaffolds can release growth factor within an optimal dosing window to effectively promote chondrogenesis of stem cells.<sup>[7]</sup> Further studies are required to identify the optimal concentration of TGF- $\beta$  that needs to be added to cartilage ECM-derived scaffolds to promote robust differentiation of embedded cells. Given previous studies which suggest that such cartilage ECM derived materials may be chondro-inductive suggests that only

relatively low levels of growth factor may need to be added to these scaffolds to facilitate the development of hyaline cartilage.<sup>[8, 9, 11, 32]</sup>

Cartilage ECM-derived scaffolds **were found to** support chondrogenesis of culture expanded infrapatellar fat pad derived stem cells *in vivo*. Cell free scaffolds were infiltrated by host cells, however when compared with stem cell seeded groups a more fibrous or fibrocartilaginous tissue was generated. This is in agreement with previous studies which demonstrate that stem cell seeded constructs promote superior matrix formation in a similar *in vivo* model.<sup>[33]</sup> In the context of developing a single-stage therapy for cartilage repair, freshly isolated CD44<sup>+</sup> infrapatellar fat pad derived stromal cells were also found to generate a cartilage-like tissue *in vivo* when seeded onto a cartilage ECM derived scaffold. Enrichment of **stromal**/stem cells based on specific cell surface markers (e.g. CD44, CD90 and CD105) has gained increased attention for tissue engineering and regenerative medicine applications.<sup>[34]</sup> CD44 is the principal cell surface receptor for hyaluronate, a key component of articular cartilage, making it an interesting target for isolating cell populations with a strong chondrogenic potential.<sup>[35]</sup> CD44 antibody-beads have previously been used for stem cell isolation and delivery, and such complexes have been shown to effectively generate chondrogenic matrix in monolayer and 3D culture.<sup>[36]</sup> A key finding of this study is that CD44 antibody enrichment can also be used to help isolate a large population of chondro-progenitor cells from freshly digested infrapatellar fat pad, a tissue known to contain an abundant number of stromal cells with a high expression of CD44.<sup>[37]</sup> Critically, this freshly isolated CD44<sup>+</sup> subset from the fat pad **appeared to** undergo comparable chondrogenesis *in vivo* to culture expanded FPSCs when seeded onto cartilage ECM derived scaffolds. Such a strategy for the enrichment and chondrogenic differentiation of freshly isolated

stromal cells will be of crucial importance for the development of single-stage procedures for cartilage regeneration.

## 5. CONCLUSION

In conclusion, this study describes a robust method to control the composition and porosity of cartilage ECM-derived scaffolds, a biomaterial with potent pro-chondrogenic properties. By seeding such a scaffold with either culture expanded infrapatellar fat pad derived stem cells, or freshly isolated CD44<sup>+</sup> stromal cells, it was possible to promote the development of a cartilage-like tissue *in vivo*. This latter finding supports the concept that enriched populations of freshly isolated stromal cells, when combined with a chondro-inductive scaffold, can induce cartilage formation and can potentially be used in one-step or single-stage procedures for cartilage repair. The clinical realisation of such a strategy would overcome many of the limitations believed to be hampering the widespread clinical adoption of current cell-based approaches such as autologous chondrocyte implantation.

## 6. ACKNOWLEDGMENTS

Funding for this study was provided by a European Research Council Starter Grant (StemRepair – Project number: 258463) and Programme for Research in Third-Level Institutions (PRTL) - Graduate Research Education Programme in Engineering.

## 7. REFERENCES

- [1] K. E. M. Benders, P. R. v. Weeren, S. F. Badylak, D. B. F. Saris, W. J. A. Dhert, J. Malda, *Trends in Biotechnology*, **2013**, 31, 169.
- [2] D. T. Felson, *New England Journal of Medicine*, **2006**, 354, 841.

- [3] a) S. D. Gillogly, M. Voight, T. Blackburn, *The Journal of orthopaedic and sports physical therapy*, **1998**, 28, 241; b) M. Brittberg, *Injury*, **2008**, 39 Suppl 1, S40.
- [4] a) W. J. F. M. Jurgens, A. van Dijk, B. Z. Doulabi, F. B. Niessen, M. J. P. F. Ritt, F. J. van Milligen, M. N. Helder, *Cytotherapy*, **2009**, 11, 1052; b) W. J. Jurgens, R. J. Kroeze, R. A. Bank, M. J. Ritt, M. N. Helder, *Journal of orthopaedic research : official publication of the Orthopaedic Research Society*, **2011**, 29, 853; c) J. E. Bekkers, L. B. Creemers, A. I. Tsuchida, M. H. van Rijen, R. J. Custers, W. J. Dhert, D. B. Saris, *Osteoarthritis and cartilage / OARS, Osteoarthritis Research Society*, **2013**, 21, 950; d) J. E. Bekkers, A. I. Tsuchida, M. H. van Rijen, L. A. Vonk, W. J. Dhert, L. B. Creemers, D. B. Saris, *The American journal of sports medicine*, **2013**, 41, 2158; e) M. Ahearne, Y. Liu, D. J. Kelly, *Tissue engineering. Part A*, **2014**, 20, 930.
- [5] C. R. Rowland, D. P. Lennon, A. I. Caplan, F. Guilak, *Biomaterials*, **2013**, 34, 5802.
- [6] S. F. Badylak, *Biomaterials*, **2007**, 28, 3587.
- [7] H. V. Almeida, Y. Liu, G. M. Cunniffe, K. J. Mulhall, A. Matsiko, C. T. Buckley, F. J. O'Brien, D. J. Kelly, *Acta Biomaterialia*, **2014**.
- [8] N. C. Cheng, B. T. Estes, H. A. Awad, F. Guilak, *Tissue engineering. Part A*, **2009**, 15, 231.
- [9] N. C. Cheng, B. T. Estes, T. H. Young, F. Guilak, *Regen Med*, **2011**, 6, 81.
- [10] a) N. C. Cheng, B. T. Estes, T. H. Young, F. Guilak, *Tissue engineering. Part A*, **2013**, 19, 484; b) J. S. Choi, B. S. Kim, J. Y. Kim, J. D. Kim, Y. C. Choi, H. J. Yang, K. Park, H. Y. Lee, Y. W. Cho, *Journal of biomedical materials research. Part A*, **2011**, 97, 292; c) B. O. Diekman, C. R. Rowland, D. P. Lennon, A. I.



- Caplan, F. Guilak, *Tissue engineering. Part A*, **2010**, 16, 523; d) K. E. M. Benders, W. Boot, S. M. Cokelaere, P. R. Van Weeren, D. Gawlitta, H. J. Bergman, D. B. F. Saris, W. J. A. Dhert, J. Malda, *Cartilage*, **2014**, 5, 221.
- [11] A. J. Sutherland, G. L. Converse, R. A. Hopkins, M. S. Detamore, *Advanced Healthcare Materials*, **2014**, n/a.
- [12] H. Madry, A. Rey-Rico, J. K. Venkatesan, B. Johnstone, M. Cucchiaroni, *Tissue engineering. Part B, Reviews*, **2014**, 20, 106.
- [13] F. J. O'Brien, B. A. Harley, M. A. Waller, I. V. Yannas, L. J. Gibson, P. J. Prendergast, *Technology and Health Care*, **2007**, 15, 3.
- [14] A. Matsiko, T. J. Levingstone, F. J. O'Brien, J. P. Gleeson, *Journal of the mechanical behavior of biomedical materials*, **2012**, 11, 41.
- [15] a) J. L. Dragoo, B. Samimi, M. Zhu, S. L. Hame, B. J. Thomas, J. R. Lieberman, M. H. Hedrick, P. Benhaim, *Journal of Bone and Joint Surgery - Series B*, **2003**, 85, 740; b) M. Q. Wickham, G. R. Erickson, J. M. Gimble, T. P. Vail, F. Guilak, *Clin Orthop Relat Res*, **2003**, 196; c) Y. Liu, C. T. Buckley, H. Almeida, K. Mulhall, D. J. Kelly, *Tissue engineering. Part A*, **2014**; d) Y. Liu, C. T. Buckley, R. Downey, K. J. Mulhall, D. J. Kelly, *Tissue engineering. Part A*, **2012**, 18, 1531; e) T. Vinardell, E. J. Sheehy, C. T. Buckley, D. J. Kelly, *Tissue engineering. Part A*, **2012**, 18, 1161; f) T. Vinardell, C. T. Buckley, S. D. Thorpe, D. J. Kelly, *Journal of Tissue Engineering and Regenerative Medicine*, **2011**, 5, 673; g) T. Mesallati, C. T. Buckley, D. J. Kelly, *Biotechnology and Bioengineering*, **2014**, 111, 1686; h) C. T. Buckley, T. Vinardell, D. J. Kelly, *Osteoarthritis and Cartilage*, **2010**, 18, 1345; i) F. He, M. Pei, *Journal of Tissue Engineering and Regenerative Medicine* 2013, 7, 73; j) K. Ye, R. Felimban, K. Traianedes, S. E. Moulton, G. G. Wallace, J. Chung, A. Quigley, P. F. M. Choong, D. E. Myers, *PLoS ONE*, **2014**, 9.

- [16] C. T. Buckley, T. Vinardell, S. D. Thorpe, M. G. Haugh, E. Jones, D. McGonagle, D. J. Kelly, *Journal of Biomechanics*, **2010**, *43*, 920.
- [17] M. G. Haugh, C. M. Murphy, R. C. McKiernan, C. Altenbuchner, F. J. O'Brien, *Tissue Engineering. Part A*, **2011**, *17*, 1201.
- [18] L. H. H. Olde Damink, P. J. Dijkstra, M. J. A. Van Luyn, P. B. Van Wachem, P. Nieuwenhuis, J. Feijen, *Biomaterials*, **1996**, *17*, 679.
- [19] O. Guillaume, A. Daly, K. Lennon, J. Gansau, S. F. Buckley, C. T. Buckley, *Acta Biomaterialia*, **2014**, *10*, 1985.
- [20] N. Y. Ignat'eva, N. A. Danilov, S. V. Averkiev, M. V. Obrezkova, V. V. Lunin, E. N. Sobol, *Journal of Analytical Chemistry*, **2007**, *62*, 51.
- [21] C. T. Buckley, D. J. Kelly, *Journal of the mechanical behavior of biomedical materials*, **2012**, *11*, 102.
- [22] D. Vonwil, D. Wendt, S. Ströbel, H. J. Wallny, D. Gygax, M. Heberer, I. Martin, *Biochemical Engineering Journal*, **2008**, *39*, 586.
- [23] F. J. O'Brien, B. A. Harley, I. V. Yannas, L. J. Gibson, *Biomaterials*, **2005**, *26*, 433.
- [24] S. F. Badylak, T. W. Gilbert, *Seminars in Immunology*, **2008**, *20*, 109.
- [25] T. K. Sampath, A. H. Reddi, *The Journal of cell biology*, **1984**, *98*, 2192.
- [26] a) S. Yang, K. F. Leong, Z. Du, C. K. Chua, *Tissue Eng*, **2001**, *7*, 679; b) Q. P. Pham, U. Sharma, A. G. Mikos, *Biomacromolecules*, **2006**, *7*, 2796.
- [27] G. I. Im, J. Y. Ko, J. H. Lee, *Cell Transplant*, **2012**, *21*, 2397.
- [28] P. Duan, Z. Pan, L. Cao, Y. He, H. Wang, Z. Qu, J. Dong, J. Ding, *Journal of biomedical materials research. Part A*, **2013**.

- [29] S. L. Voytik-Harbin, A. O. Brightman, M. R. Kraine, B. Waisner, S. F. Badylak, J. *Cell Biochem*, **1997**, *67*, 478.
- [30] L. D. Solorio, E. L. Vieregge, C. D. Dhimi, P. N. Dang, E. Alsberg, *Journal of Controlled Release*, **2012**, *158*, 224.
- [31] a) A. N. Buxton, C. S. Bahney, J. U. Yoo, B. Johnstone, *Tissue engineering. Part A*, **2011**, *17*, 371; b) B. A. Byers, R. L. Mauck, I. E. Chiang, R. S. Tuan, *Tissue engineering. Part A*, **2008**, *14*, 1821; c) C. Chung, J. A. Burdick, *Tissue engineering. Part A*, **2009**, *15*, 243.
- [32] B. O. Diekman, B. T. Estes, F. Guilak, *Journal of biomedical materials research. Part A*, **2010**, *93*, 994.
- [33] T. Re'em, Y. Kaminer-Israeli, E. Ruvinov, S. Cohen, *Biomaterials*, **2012**, *33*, 751.
- [34] a) S. M. Mihaila, A. K. Gaharwar, R. L. Reis, A. Khademhosseini, A. P. Marques, M. E. Gomes, *Biomaterials*, **2014**, *35*, 9087; b) T. Rada, R. Reis, M. Gomes, *Stem Cell Reviews and Reports*, **2011**, *7*, 64; c) B. Levi, D. C. Wan, J. P. Glotzbach, J. Hyun, M. Januszyk, D. Montoro, M. Sorkin, A. W. James, E. R. Nelson, S. Li, N. Quarto, M. Lee, G. C. Gurtner, M. T. Longaker, *The Journal of biological chemistry*, **2011**, *286*, 39497; d) M. T. Chung, C. Liu, J. S. Hyun, D. D. Lo, D. T. Montoro, M. Hasegawa, S. Li, M. Sorkin, R. Rennert, M. Keeney, F. Yang, N. Quarto, M. T. Longaker, D. C. Wan, *Tissue engineering. Part A*, **2013**, *19*, 989; e) M. C. Arufe, M. C. De La Fuente, I. Fuentes-Boquete, F. J. De Toro, F. J. Blanco, *Journal of Cellular Biochemistry*, **2009**, *108*, 145.
- [35] A. Aruffo, I. Stamenkovic, M. Melnick, C. B. Underhill, B. Seed, *Cell*, **1990**, *61*, 1303.

- [36] a) S. Yanada, M. Ochi, N. Adachi, H. Nobuto, M. Agung, S. Kawamata, *Journal of Biomedical Materials Research - Part A*, **2006**, 77, 773; b) M. Motoyama, M. Deie, A. Kanaya, M. Nishimori, A. Miyamoto, S. Yanada, N. Adachi, M. Ochi, *Journal of Biomedical Materials Research - Part A*, **2010**, 92, 196.
- [37] W. S. Khan, A. B. Adesida, S. R. Tew, U. G. Longo, T. E. Hardingham, *Cell Prolif*, **2012**, 45, 111.

## 8. FIGURES

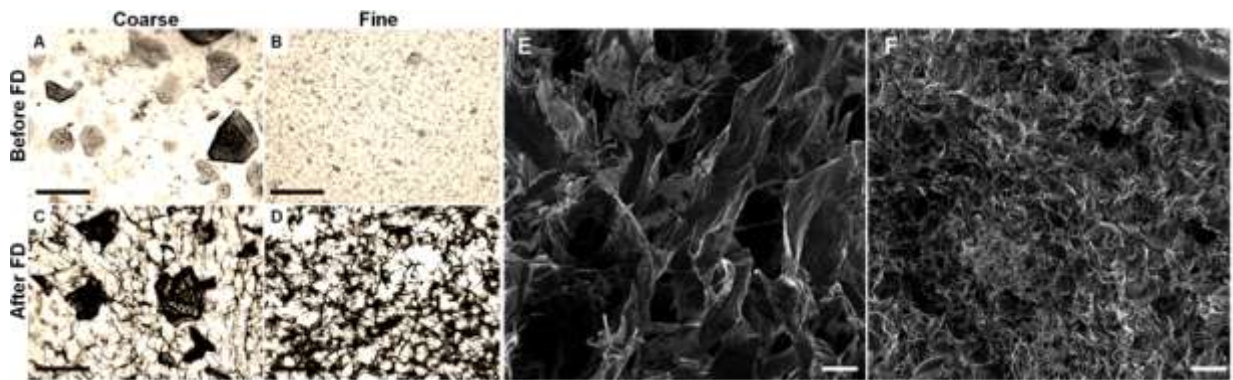


Figure 1 – Light micrographs of cartilage slurries: coarse (A, C) and fine (B, D) before and after freeze-drying (FD) (scale bar: 500  $\mu$ m). Helium ion micrographs of cartilage ECM-derived scaffolds produced using either a coarse (E) and fine (F) slurry (scale bar: 100  $\mu$ m).

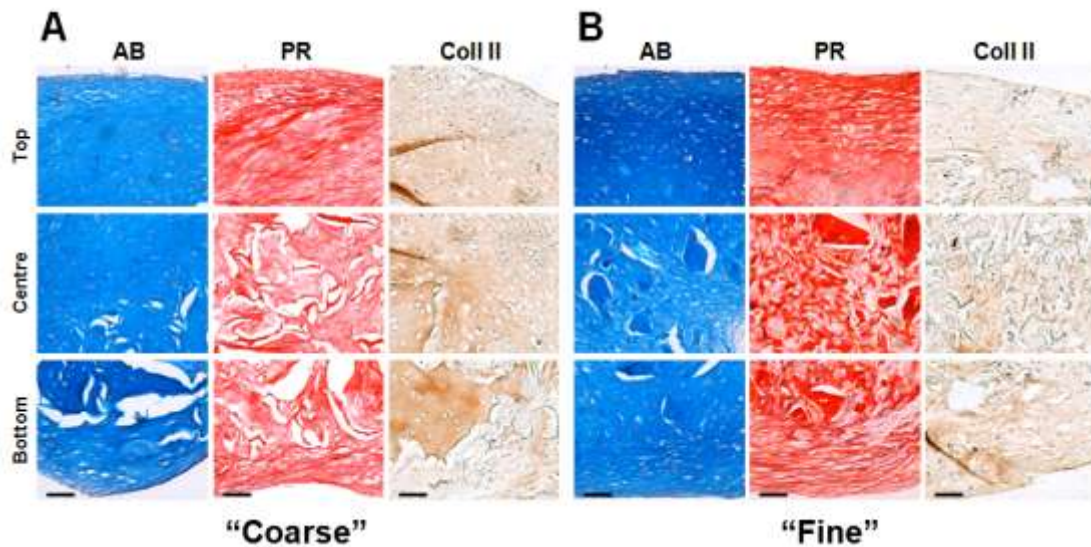


Figure 2 –Alcian blue (AB), picro-sirius red (PR) and collagen type II (Coll II) staining of ECM-derived scaffold produced using a coarse (A) or fine (B) slurry, after 28 days of culture (scale bar: 50 $\mu$ m).

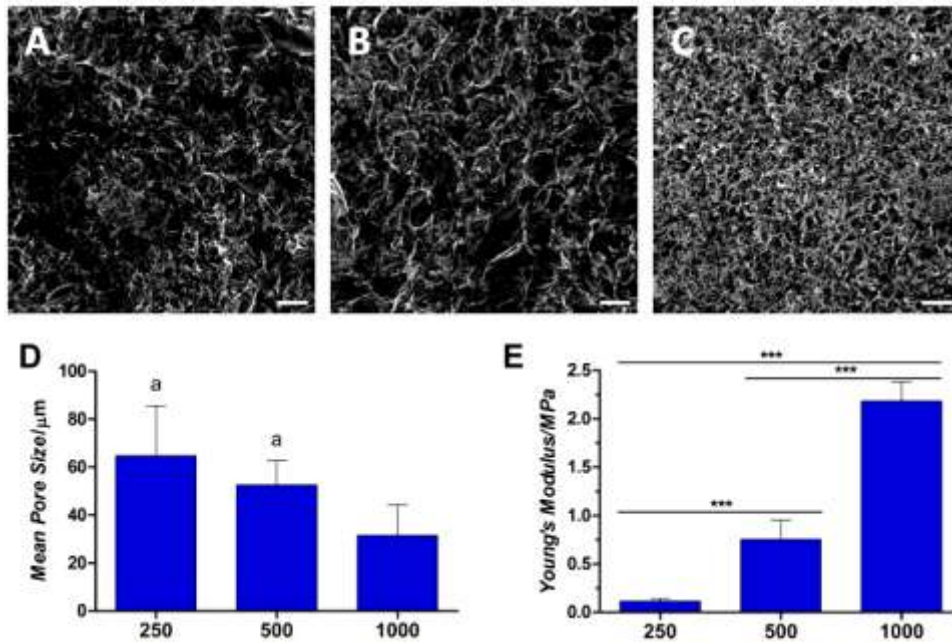


Figure 3 – (A-C) Helium ion microscopy (HIM) micrographs of scaffolds with altered cartilage ECM slurry concentrations: (A) 250 mg/ml; (B) 500 mg/ml; (C) 1000 mg/ml scaffolds (scale bar: 100 µm). (D) Mean scaffold pore size (<sup>a</sup> $p < 0.05$ ; *a* indicates a significant difference to the 1000 mg/ml group). (E) Young's Modulus for each dry scaffold at day 0 ( $n=3$ ; <sup>\*\*\*</sup> $p < 0.001$ ).

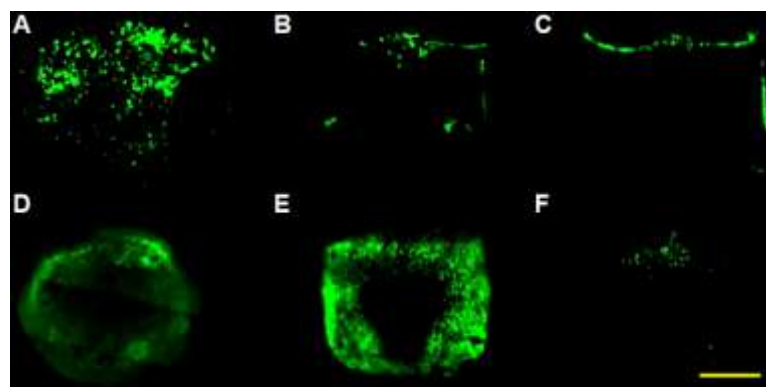


Figure 4 – (A-C) Confocal microscopy at day 1 of human infrapatellar fat pad derived stem cells seeded in ECM-derived scaffolds; calcein was used to stain live cells: (A) 250 mg/ml, (B) 500 mg/ml and (C) 1000 mg/ml. (D-F) Scaffolds at day 28: (D) 250 mg/ml, (E) 500 mg/ml and (F) 1000 mg/ml scaffolds. Images represent a cross-section through ECM-derived constructs (scale bar: 2 mm).

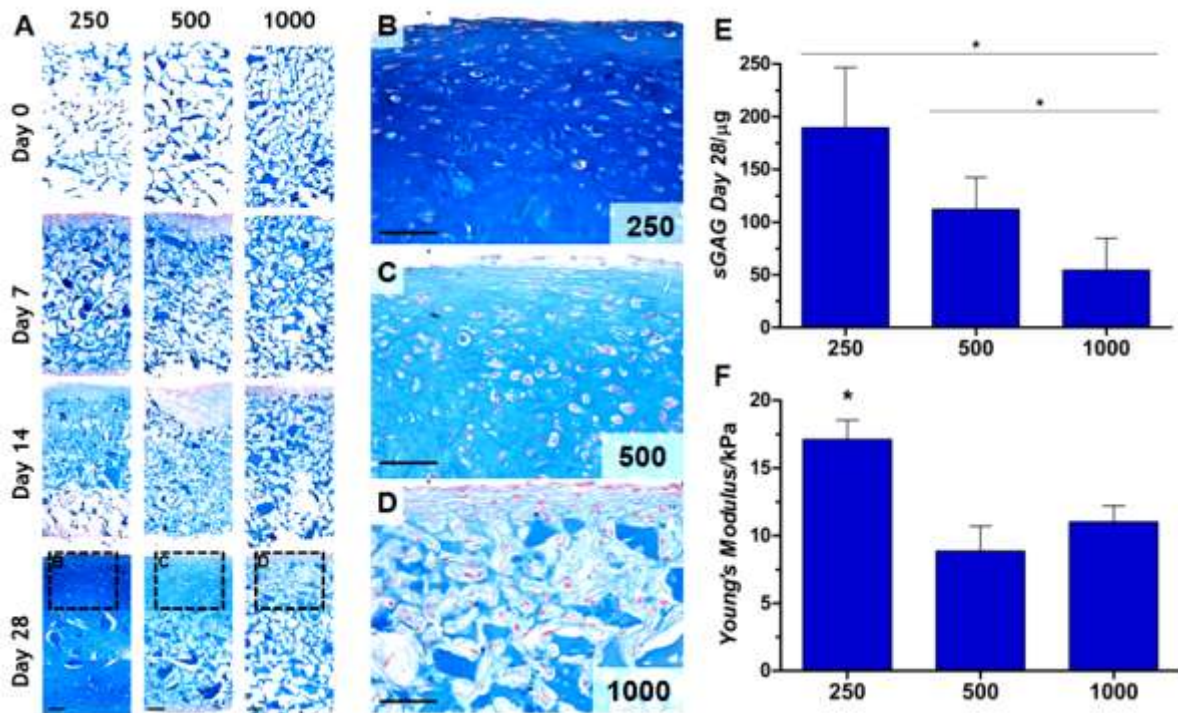


Figure 5 – Histological sections staining for glycosaminoglycans (sGAG) (alcan blue) and cell *nuclei* (nuclear fast red) in 250, 500 and 1000 mg/ml ECM-derived scaffolds (seeded with FPSCs) at day 0, 7, 14 and 28 of culture (A). (B-D) High magnification images demonstrating more robust sGAG deposition within the 250 mg/ml scaffolds (B) compared to the 500 (C) 1000 mg/ml (D) scaffolds (scale bar: 50  $\mu$ m). sGAG accumulation for day 28 (E) and Young's modulus for day 28 (F), within the 250, 500 and 1000 mg/ml scaffolds (n=4, \* $p$ <0.05).

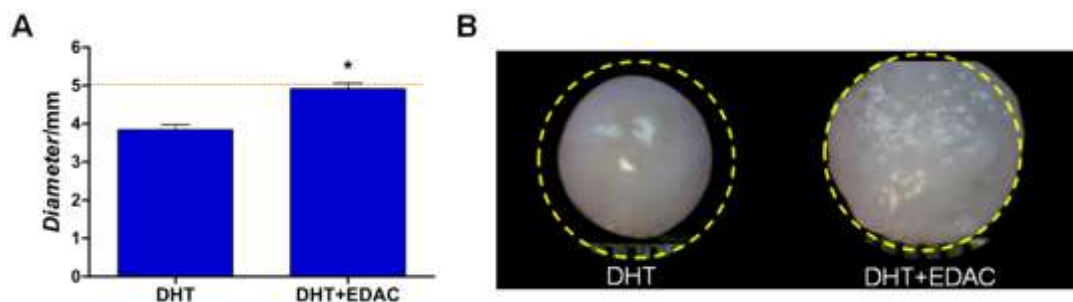


Figure 6 – (A) Diameter of ECM-derived scaffolds that had been crosslinked with DHT or DHT and EDAC after 28 days in culture (n=4, \* $p$ <0.05). (B) Macroscopic images of scaffolds (yellow represents initial diameter: 5 mm).

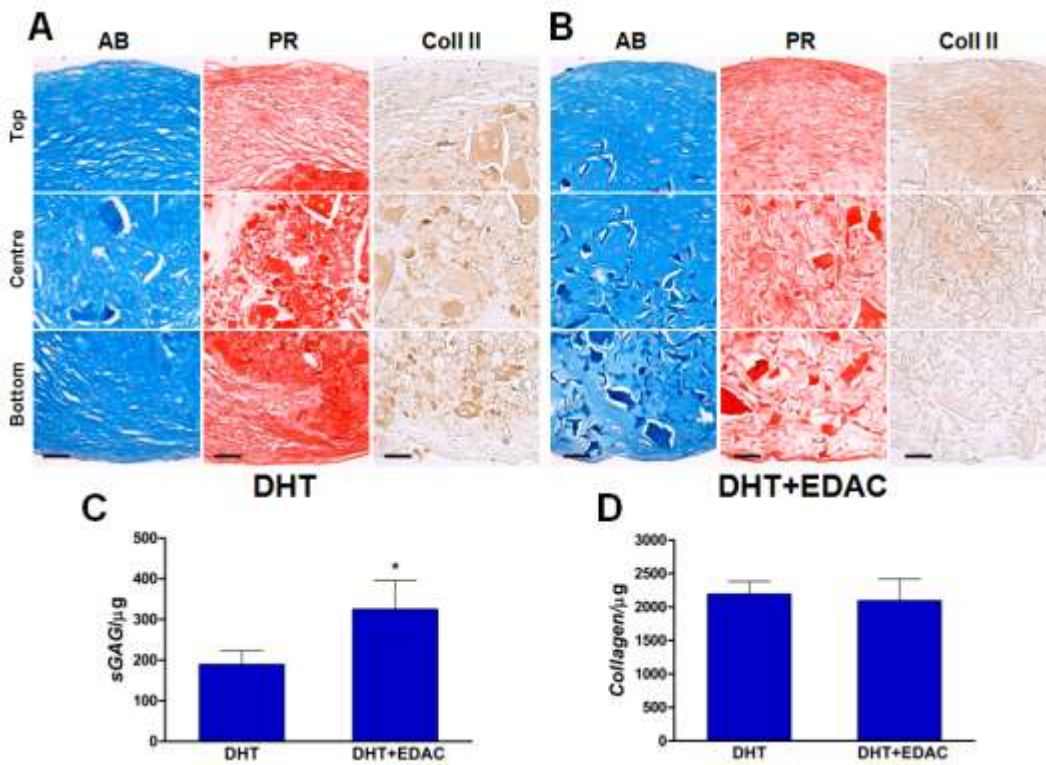


Figure 7 – Alcian blue (AB), picro-sirius red (PR) and collagen type II (Coll II) staining of ECM-derived scaffolds after 28 days of culture. (A) Dehydrothermal (DHT) crosslinking; (B) DHT + 1-Ethyl-3-(3-dimethyl aminopropyl) carbodiimide (EDAC) crosslinking (scale bar: 50  $\mu$ m). (C) sGAG and (D) collagen accumulation within DHT and DHT+EDAC crosslinked ECM-derived scaffolds seeded with human FPSCs (n=4, \* $p$ <0.05).



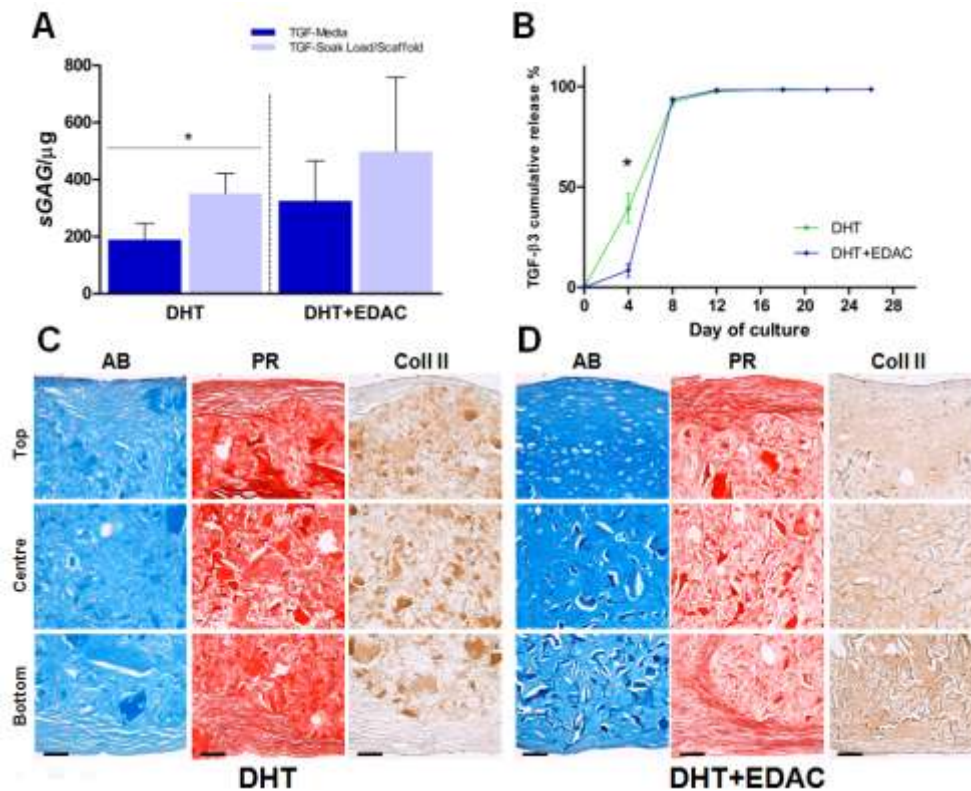


Figure 8 – (A) sGAG accumulation after 28 days in culture for scaffolds soak-loaded with TGF-β3 (TGF-soak load/scaffold) compared to constructs where TGF-β3 was added to the media (TGF-media) Scaffolds with and without EDAC crosslinking were analysed (n=4, \* $p < 0.05$ ). (B) TGF-β3 release into the media from TGF-β3 loaded ECM-derived scaffold with and without EDAC crosslinking (n=6, \* $p < 0.05$ ). (C, D) Alcian blue (AB), picro-sirius red (PR) and collagen type II (Coll II) staining of ECM-derived scaffold loaded with TGF-β3 for DHT (C) and DHT+EDAC (D) crosslinked scaffolds after 28 days of culture (scale bar: 50μm).

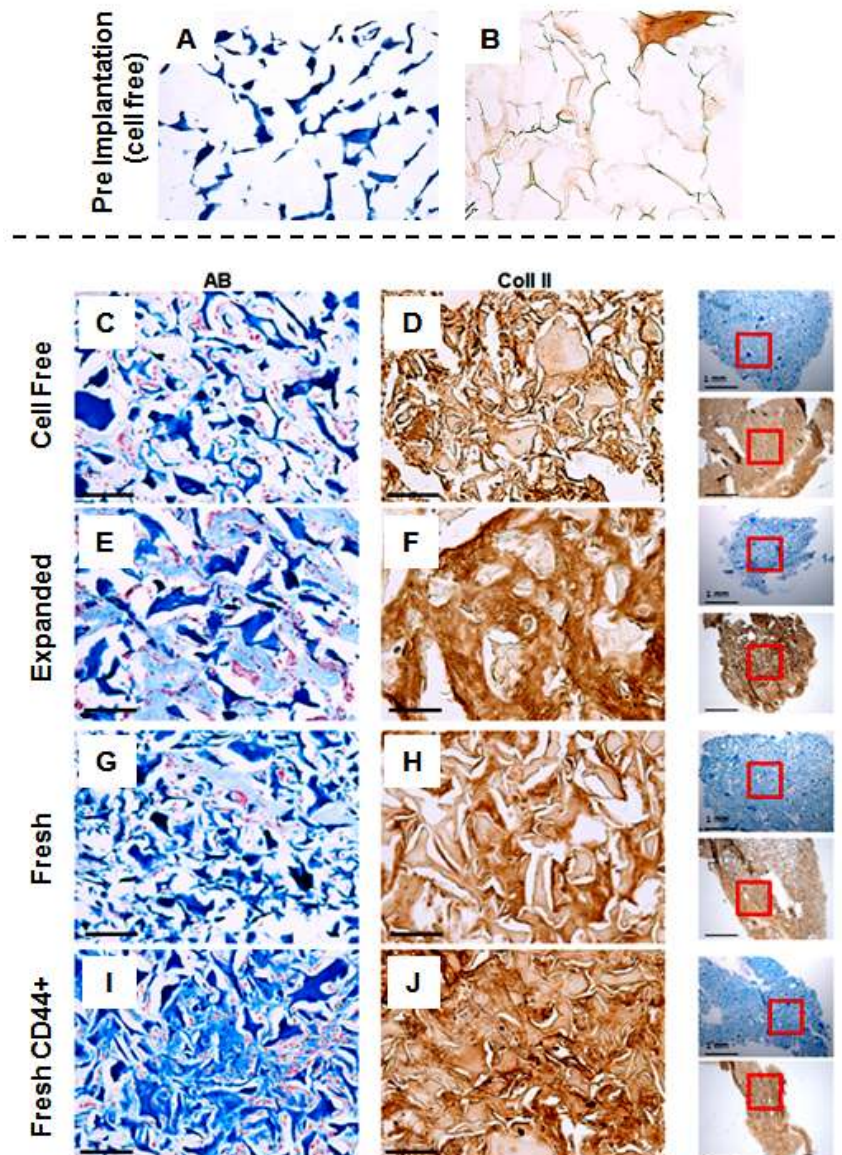


Figure 9 – Alcian blue (AB) and collagen type II (Coll II) histological staining for day 0 before implantation (A and B), implanted cell free scaffolds (C and D respectively), expanded FPSC seeded constructs (E and F), freshly isolated fat pad stromal cell seeded constructs (G and H) and freshly isolated CD44<sup>+</sup> stromal cell seeded constructs (I and J). All groups were implanted *in vivo* for four weeks (scale bar: 50µm).